Electrical, Control and Communication Engineering

ISSN 2255-9159 (online)
ISSN 2255-9140 (print)
2017, vol. 12, pp. 27–33
doi: 10.1515/ecce-2017-0004
https://www.degruyter.com/view/j/ecce

Energy Scheduling of Battery Storage Systems in Micro Grids

Andreas Armstorfer* (*Researcher, University of Applied Sciences Kempten*), Helmuth Biechl (*Director, IEES*), Argo Rosin (*Senior Research Scientist, Tallinn University of Technology*)

Abstract **– Microgrids in island mode with high penetration of renewable energy sources in combination with gensets and battery storage systems need a control system for voltage and frequency. In this study the main goal is maximization of the energy feed-in by renewable sources. Therefore it is necessary to keep the State of Energy for the Battery Storage System in a range that the excess energy can be absorbed and used in a later period of the day. In this paper an approach for State of Charge scheduling based on load and generation prediction is described.**

Keywords **– Distributed power generation; Energy storage; Islanding; Microgrids; Power system management.**

I. Introduction

In island grids with volatile renewable power generation it is desired that this sources can always feed in their maximum power.

The usage of battery storage systems (BSS) can support the grid, especially when the renewable generation is higher than the power consumption. In these periods the excess energy has to be absorbed completely by the BSS, as gensets can only deliver power. It has to be ensured that the State of Energy (SOE) of the BSS do not exceed its limits and always have enough margin. In this paper we work with the State of Energy (SOE) instead of the State of Charge (SOC) which slightly differs due to the changing voltage. The approach for BSS scheduling given here is based on the prediction of load and renewable power generation.

In periods of excess electricity generation, the BSS need to store the complete energy. Therefore the SOE has to be scheduled that way that the BSS is discharged sufficiently in periods with a lack of power. Furthermore uncertainties of prediction need to be taken into account as well.

For a stable operation with several grid-building components, frequency control is necessary. The concept presented here is based on primary and secondary control [1]–[6].

Reactive power and voltage control is not considered in this study.

II. Grid Structure

An island grid with distributed renewable energy sources (distributed power generation, DG) is investigated. It is assumed that all DG units are current sources without grid building capability. Furthermore directly coupled gensets (e.g. driven by vegetable oil) and Battery Storage Systems (BSS) are available. The complete system is monitored and controlled by a microgrid controller (MGC). In Fig. 1, the investigated grid structure is illustrated.

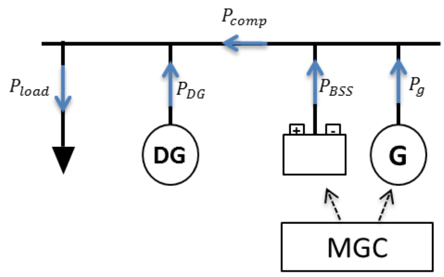

Fig. 1. Island grid consisting of consumers (load), distributed renewable energy sources (DG), gensets, battery storage systems (BSS) and a microgrid controller (MGC).

The active power consumption of the grid is summarized to P_{load} whereas P_{DG} is the sum of all DG. For an equilibrium of power, the compensation power P_{comp} is introduced:

$$P_{\text{comp}} = P_{\text{load}} - P_{\text{DG}}. \tag{1}$$

The power deviation is compensated by gensets (P_{g}) as well as Battery Storage Systems (P_{BSS}):

$$P_{\text{comp}} = P_{\text{g}} + P_{\text{BSS}}. \tag{2}$$

For grid building and frequency control, at least one genset resp. BSS must be in operation. For load sharing, the conventional concept of primary and secondary control is used. For active power sharing, the following dependency between active power and frequency is implemented:

$$P_\nu(f) = P_{0,\nu} - k_{f,\nu} \cdot (f - f_{0,\nu}) \tag{3}$$

where $f_{0,\nu}$ and $P_{0,\nu}$ are the setpoints for frequency and power for each component ν. The frequency droop factor $k_{f,\nu}$ defines the relation between active power and frequency deviation.

For primary control, the second part of the relation shown in (3), $k_{f,\nu}(f - f_{0,\nu})$ is responsible to stabilize the grid. Depending

* Corresponding author.
E-mail: andreas.armstorfer@hs-kempten.de

on the droop factor $k_{f,\nu}$ active power is supplied for a certain frequency deviation. As this control needs to react very fast, it is implemented directly in the component controller. A load depending frequency deviation is acceptable.

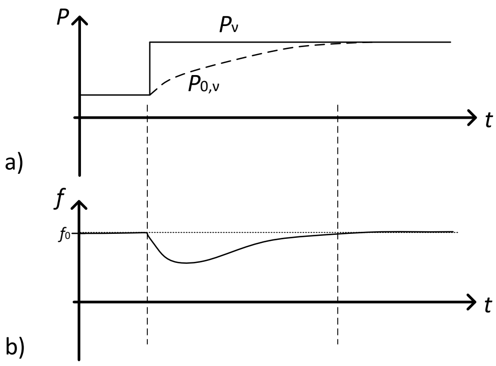

Fig. 2. Primary and secondary control; a) active power and active power setpoint; b) grid frequency.

The secondary control is changing the setpoint $P_{0,\nu}$ with a slow time constant to reach the original frequency again (Fig. 2).

III. Secondary Control

Besides primary control, the active power setpoint $P_{0,\nu}$ of each component ν is set by the secondary control which is much slower than the primary control. In the study presented in this paper, $P_{0,\nu}$ is based on load and DG prediction.

For dimensioning of the control system, several conditions are defined:

- It is assumed that the consumed energy per day is higher than the energy produced by DG:

$$\int_0^{T_{end}} P_{comp}(t')dt' > 0 \tag{4}$$

whereas $T_{\text{end}} = 24\,\text{h}$.

- The BSS is not able to consume or generate energy for a very long time. Hence after a certain periodical time span T_{end}, e.g. 1 day, it is assumed:

$$\int_0^{T_{end}} P_{BSS}(t')dt' = 0 \tag{5}$$

$$\int_0^{T_{end}} P_{comp}(t')dt' = \int_0^{T_{end}} P_g(t')dt' \tag{6}$$

- The genset power P_{g} is always positive (no power feedback):

$$P_g \geq 0 \tag{7}$$

- It is assumed that gensets as well as BSS can feed the grid alone with respect to power, that means without renewable energy generation. Measurements in a real system show clearly that due to cloudy sky PV power as an example for DG can decrease from 80 % to 20 % within less than one minute. This fact necessitates an immediate take-over of the load by the BSS for at least a short period of time.

- The energy stored in the BSS is defined as $E_{\text{BSS}}(t)$ and depends on the initial stored energy $E_{\text{BSS},0}$ and on the integral of the BSS power:

$$E_{BSS}(t) = E_{BSS,0} - \int_0^{t} P_{BSS}(t')dt' \tag{8}$$

Self-discharge is neglected.

$P_{\text{BSS}} > 0$ if the BSS is delivering power.
Another common representation for the energy stored in a BSS is the State of Energy (SOE) [7]:

$$SOE(t) = \frac{E_{BSS}(t)}{E_{BSS,total}} \tag{9}$$

where $E_{\text{BSS,total}}$ is the total capacity of the BSS at the time of operation.

- The energy $E_{\text{BSS}}(t)$ that needs to be stored has to be in the range of :

$$E_{BSS,\min} \leq E_{BSS}(t) \leq E_{BSS,\max} \tag{10}$$

resp.

$$SOE_{\min} \leq SOE(t) \leq SOE_{\max} \tag{11}$$

IV. Microgrid Controller Setup

The MGC presented in this work is a superordinate controller for the operation of microgrid facilities (BSS, gensets) and responsible for the application planning (Fig. 3).

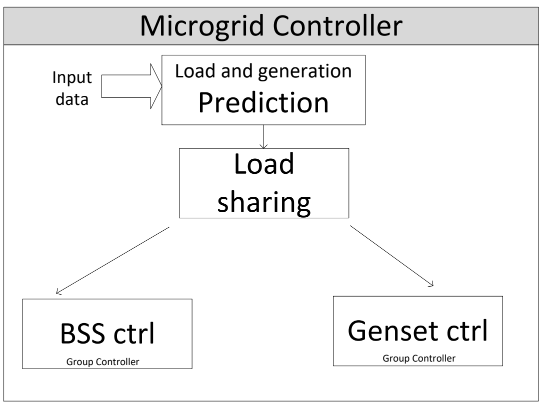

Fig. 3. Structure of the microgrid controller (MGC).

The MGC consists of group controllers for BSS and gensets as well as a block for load sharing between BSS and gensets. As a fundamental for load sharing planning, the electrical consumption (load) and the volatile DG production are predicted (prediction block). As the DG sources have no grid building capability, at least one BSS or genset must always be in operation.

A. Prediction

The power consumption P_{load} as well as the volatile electricity generation P_{DG} are predicted. Many conditions and effects need to be taken into account. In the literature several methods are described [8]–[13], but this subject is not part of this study. Thus a prediction of the compensation power P_{comp} can be determined according to (1). At times of higher production than consumption (P_{comp} negative), the BSS must be capable to store the excess energy. Therefore it needs to be ensured that the stored energy is within the limits defined in (10) resp. (11).

B. Load Sharing Planning

The difference between P_{load} (consumption) and P_{DG} (volatile generation) needs to be compensated by the gensets and/or the BSS.

For the compensation power P_{comp} it has to be distinguished between sections where $P_{\text{comp}} \geq 0$ and where $P_{\text{comp}} < 0$. Therefore the predicted curve P_{comp} is divided into i different sections. The borders t_i of the sections are determined by a zero-crossing method. The energy of each section can be calculated by:

$$E_i = \int_{t_{i-1}}^{t_i} P_{comp}(t')dt' \tag{12}$$

Fig. 4a shows an example for the predicted curve P_{comp}. It can be divided up into 5 sections. In the first, third and fifth, P_{comp} is positive. In section two and four it is negative, that means that power needs to be absorbed. As gensets cannot absorb power (7), the BSS need to be charged. It has to be ensured that the BSS always have enough free capacity. In other words the SOE needs to be small enough before the charging period. The amount of energy in the 5 sections is calculated to $E_1, \ldots, E_5$.

For this reason, at the time t_1 resp. t_3 the BSS must have enough residual capacity to store the energy E_2 resp. E_4. Under consideration of (10), the following conditions must be fulfilled (Fig. 4b):

$$E_{BSS,\min} \leq E_{BSS}(t_1) \leq E_{BSS,\max} - E_2 \tag{13}$$

$$E_{BSS,\min} \leq E_{BSS}(t_3) \leq E_{BSS,\max} - E_4 \tag{14}$$

Consequently, at the time t_2 resp. t_4 the stored energy of the BSS $E_{\text{SOC}}(t)$ is in the range of:

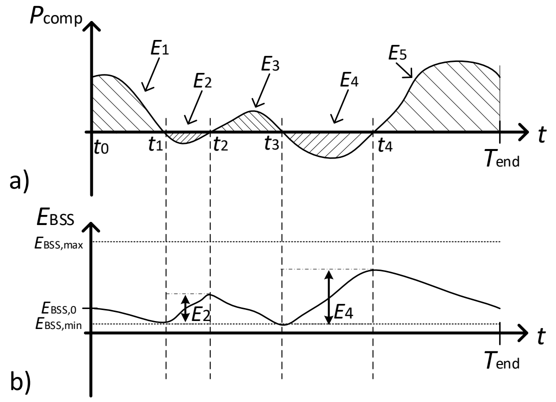

Fig. 4. Example for compensation power and the related stored energy of the BSS.

$$E_{BSS,\min} + E_2 \leq E_{BSS}(t_2) \leq E_{BSS,\max} \tag{15}$$

$$E_{BSS,\min} + E_4 \leq E_{BSS}(t_4) \leq E_{BSS,\max} \tag{16}$$

As a general approach for (13)–(16), $E_{\text{BSS}}(t_i)$ at the beginning of the charging period needs to be in the range of:

$$E_{BSS,\min} \leq E_{BSS}(t_i) \leq E_{BSS,\max} - E_{i+1} \tag{17}$$

After charging periods, $E_{BSS}(t_i)$ is in the range of:

$$E_{BSS,\min} + E_i \leq E_{BSS}(t_i) \leq E_{BSS,\max} \tag{18}$$

As maximum renewable energy feed-in is one main goal, the BSS should always be able to store the excess energy completely. Thus it is necessary to keep the SOE at a low level, as low as possible but as high as necessary to fulfill the required demands of the following periods. Before a period in which the BSS will be charged, the SOE should be at $SOE_{\min}$.

Besides this, at the time $t = 0$ the curve for E_{BSS} is defined to:

$$E_{BSS}(t=0) = E_{BSS,0} \tag{19}$$

Depending on (2) and (5), at time the $t = T_{\text{end}}$ the value of E_{BSS} should reach again $E_{\text{BSS,0}}$:

$$E_{BSS}(t=T_{end}) = E_{BSS,0} \tag{20}$$

Next, the power setpoint curves for the BSS $P_{\text{BSS}}(t)$ as well as for the gensets $P_{\text{g}}(t)$ are estimated.

Therefore it is distinguished between ranges of $P_{\text{comp}} \leq 0$ (case a) and $P_{\text{comp}} > 0$ (case b).

Case a) $P_{comp} \leq 0$: in times when P_{comp} is negative, no gensets are feeding in ($P_g = 0$). Hence the BSS power in this time range is equal:

$$P_{BSS}(P_{comp} \leq 0) = P_{comp} \tag{21}$$

Case b) For ranges of $P_{comp} > 0$, the load sharing depends on the predicted energy until the BSS is charged again.

Therefore the load sharing factor k_{BSS} is introduced. In the following it is defined by the share of energy that can be delivered by the BSS in the time range from t_i to t_{i+1} divided by the total compensation energy E_{comp} in the same period:

$$k_{BSS,i} = \frac{E_{BSS}(t_i) - E_{BSS,\min}(t_{i+1})}{E_{comp}(t_{i+1}) - E_{comp}(t_i)} \tag{22}$$

where t_i and t_{i+1} are the borders of the time range of a block with positive P_{comp}. In the example shown in Fig. 4 the ranges are:

- from t_0 to t_1,
- from t_2 to t_3,
- and from t_4 to T_{end}.

Before an interval in which the BSS needs to be charged according the prediction, SOE must be kept low enough, ideally at SOE_{min}. This fact defines $E_{BSS}(t_i)$ respectively $k_{BSS,i}$. In other words, it determines the participation of BSS in the load sharing. Additionally an uncertainty in both, load resp. generation prediction, must be taken into account.

If the available energy of the BSS is greater than the needed energy, $k_{BSS,i}$ is limited to:

$$0 \leq k_{BSS,i} \leq 1 \tag{23}$$

In that case, the gensets are not in operation in this interval.

This leads to the following BSS and genset power for the section i:

$$P_{BSS}(t) = k_{BSS,i} \cdot P_{comp}(t) \text{ for } t_i \leq t \leq t_{i+1}; \tag{24}$$

$$P_g(t) = (1 - k_{BSS,i}) \cdot P_{comp}(t) \text{ for } t_i \leq t \leq t_{i+1}; \tag{25}$$

Now for the whole predicted time range the BSS' SOE as well as genset and BSS power are set. If the BSS is not capable to store the excessive energy completely, further concepts like DG feed-in reduction or additional loads such as power-to-heat systems are necessary, but this is not part of the presented work.

C. Group Controllers

If more than one genset unit or BSS unit exist, a group controller is in charge of optimum operation of these components. Depending on the requested power, one or more units are in operation. Other conditions like minimum power, minimum time in operation, redundancy but also environmental aspects like noise emission can be taken into account. The dimensioning depends highly on the local circumstances where the island grid is installed and need to be adapted individually.

The group controller also allows changing of the droop factors of each unit with respect to primary control.

V. Simulation

The concept of load sharing by SOE prediction described above is simulated using the software Matlab.

It is basing on the prediction of the load P_{load} as well as of the DG P_{DG}. The prediction data have a resolution of 15 minutes for a time span of 24 hours.

It is assumed that the sum of the maximum active power of all the BSS is higher than the maximum value of P_{comp}. For $P_{comp} > 0$ the same is assumed for the gensets.

The BSS dimensioning is described in Table I, according to a real Li-Ion based storage system in the village Wildpoldsried in the south of Germany [14]–[16].

TABLE I

BSS Simulation Parameters

Total Energy Capacity	165 kWh
Max. State of Energy	0.8
Min. State of Energy	0.2
Initial SOE	0.3

In this study, 4 different scenarios are investigated by simulation. The predicted load curve P_{load} (standard load profile H0 for households) for an annual electricity demand of 560 MWh is shown in Fig. 5a.

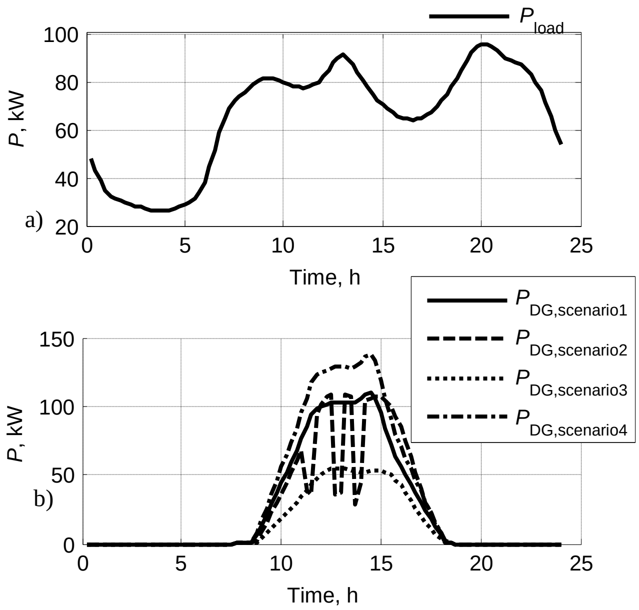

Fig. 5. a) Load prediction curve for 1 day; b) four different scenarios for the DG curve for 1 day.

Further for all assumed scenarios the DG curve (P_{DG}) can be seen in Fig. 5b. The amount of generated energy as well as the maximum power generated by DG is shown in Table II.
For each scenario, the compensation power P_{comp} is calculated out of P_{load} and P_{DG} according to (1).

TABLE II
DG CHARACTERISTICS FOR INVESTIGATED SCENARIOS

Scenario	Total Energy, kWh	Max. Power, kW
1	631.2	110.6
2	592.9	108.9
3	333.7	54.8
4	789.0	138.3

A. Scenario 1

The predicted power P_{comp} defined as the difference between P_{load} and P_{DG} has to be balanced by BSS and gensets. It is illustrated for scenario 1 in Fig. 6.

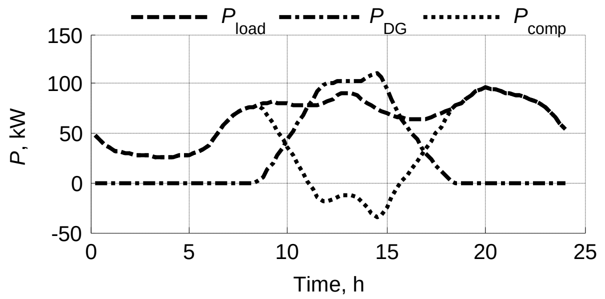

Fig. 6. Prediction curve for P_{load}, P_{DG} and the resulting P_{comp} (scenario 1).

It can be seen that the BSS has to absorb power in the time range between approx. 11h and 16h ($P_{comp} < 0$). In this time period, the genset is not in operation ($P_g = 0$). The simulation results for scenario 1 are shown in Fig. 7.

To reach SOE_{min} before the charging period, the BSS is discharged in the interval between 0h and 11h with $k_{BSS} = 0.04$. That means that approx. 4 % of P_{comp} is supplied by the BSS while 96 % is supplied by the genset. In the next period (from 11 h to 16 h), the genset is off while the BSS is charged (from $SOE = 0.2$ to $SOE = 0.7$). In the period from 16 h to 24 h, the BSS is discharged with approx. 12 % of P_{comp} to reach again the initial $SOE = 0.3$ at the time 24 h.

B. Scenario 2

For scenario 2, the resulting curve for P_{comp} is shown in Fig. 8. It is assumed that the decentralized generation has a high volatile behavior. This also effects P_{comp}.

The results for P_{BSS}, P_g and P_{comp} are shown in Fig. 9a. It can be seen clearly that the power fluctuation in the time period between 12.5h and 16h is completely covered by the BSS. The gensets are off during this period ($P_g = 0$).

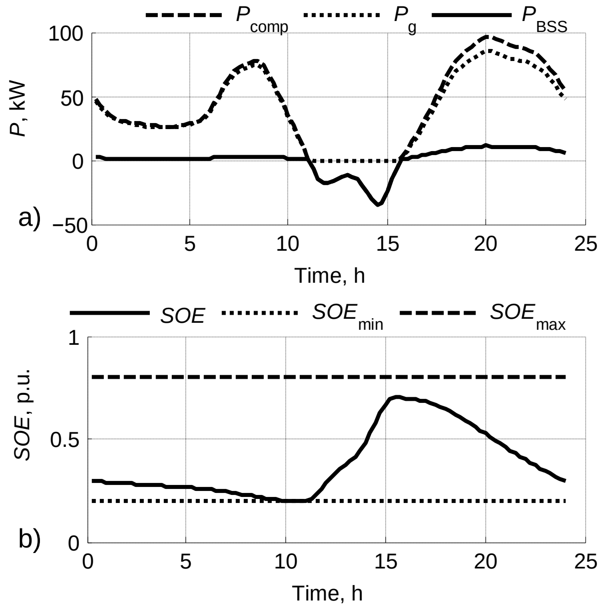

Fig. 7. a) BSS and genset power curve for 1 day. b) resulting SOE curve for scenario 1.

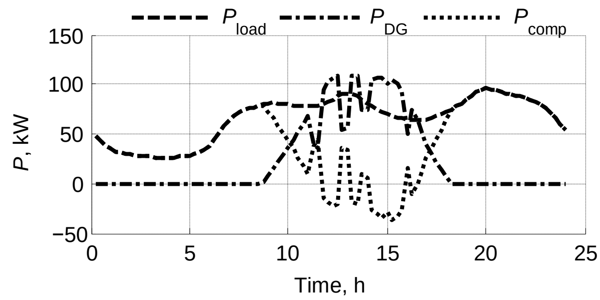

Fig. 8. Prediction curve for P_{load}, P_{DG} and the resulting P_{comp} (scenario 2).

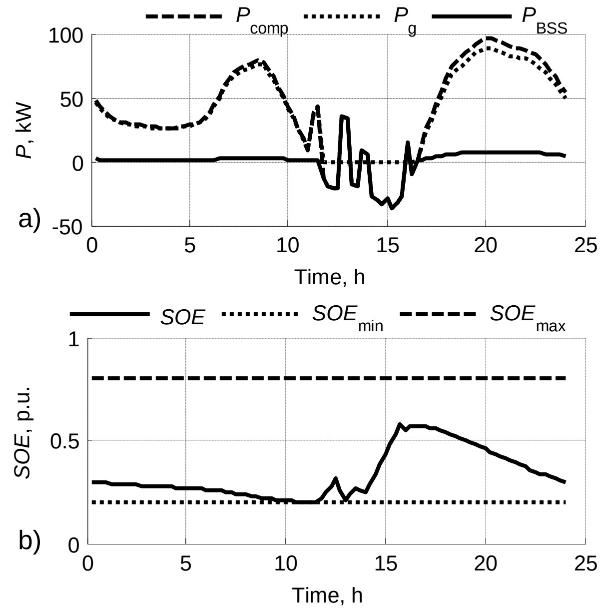

Fig. 9. a) BSS and genset power curve for 1 day. b) Resulting *SOE* curve (scenario 2).

C. Scenario 3

In scenario 3, the electrical load is always higher than the power fed in by DG (Fig. 10).

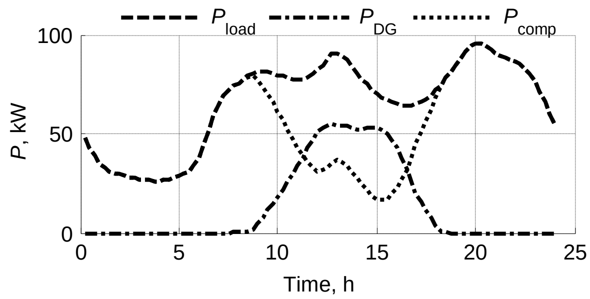

Fig. 10. Prediction curve for P_{load}, P_{DG} and the resulting P_{comp} (scenario 3).

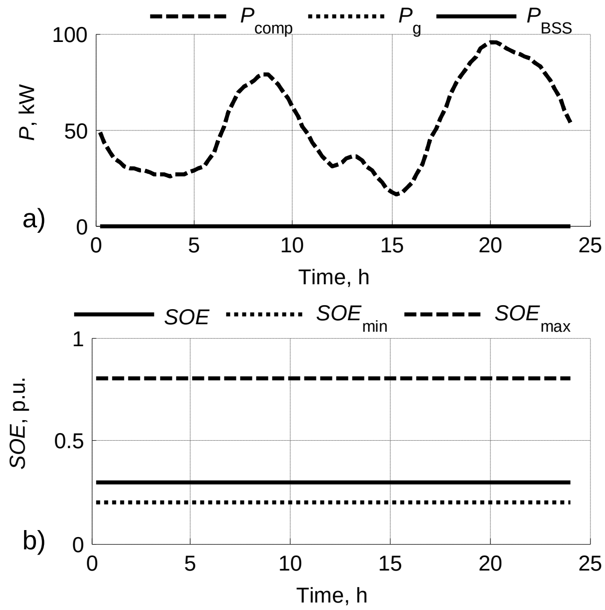

Fig. 11. a) BSS and genset power curve for 1 day. b) Resulting SOE curve (scenario 3).

Hence the renewable power is consumed by the load at all times. As the BSS cannot generate energy (2), it will not increase the amount of usable renewable energy when looking at a full day.

For that reason the BSS is not used for load sharing (Fig. 11). The predicted SOE stays constant. Nevertheless, fast changes of power (primary control) will be covered by BSS.

D. Scenario 4

In the last scenario, a high DG feed-in is assumed (Fig. 12). In Fig. 13 it can be seen that the BSS capacity is not sufficient for the predicted DG generation. At maximum, the BSS needs to store 205 kWh which is more than the rated capacity. Therefore other steps are necessary for a stable operation of the island grid. This could be for example a reduction of DG generation or the usage of further loads, such power-to-heat systems. These methods are not described in the frame of this study.

VI. Conclusion

In this study first steps of a concept for load sharing prediction and BSS scheduling in small island grids are presented. The main goal is the complete usage of the volatile renewable power generation by application of battery storage systems (BSS). All the renewable energy should be used to reduce the operation of conventional power sources such as gensets. Simulation results for SOE prediction are shown for different scenarios. Fast changes of power (primary control) are not taken into account in the simulation.

This work presents a method for optimum dimensioning and operation of batteries in non-interconnected microgrids with a high penetration of renewable energy sources.

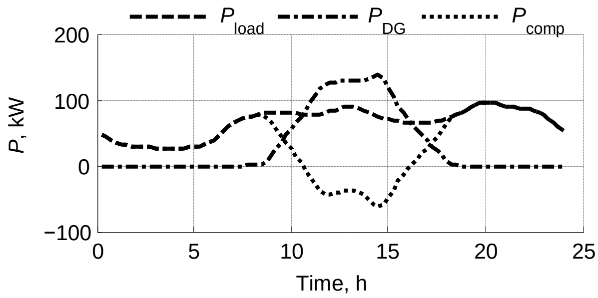

Fig. 12. Prediction curve for P_{load}, P_{DG} and the resulting P_{comp} (scenario 4).

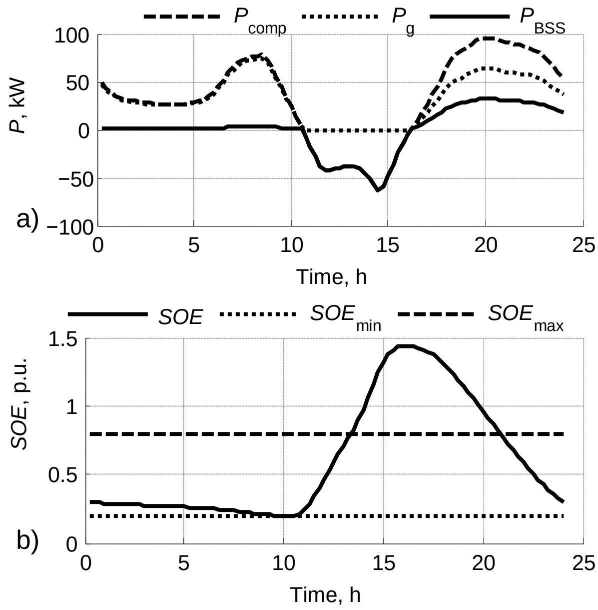

Fig. 13. a.) BSS and genset power curve for 1 day. b.) Resulting SOE curve (scenario 4).

References

[1] D. Oeding and B. Oswald, *Elektrische Kraftwerke und Netze*. 2011.

[2] A. J. Schwab, *Elektroenergiesysteme*, 3. Auflage. Springer Berlin Heidelberg, 2012.

[3] J. Rocabert, A. Luna, F. Blaabjerg, and P. Rodríguez, "Control of Power Converters in AC Microgrids," *IEEE Transactions on Power Electronics*, vol. 27, no. 11, pp. 4734–4749, Nov. 2012. https://doi.org/10.1109/tpel.2012.2199334

[4] K. De Brabandere, B. Bolsens, J. Van den Keybus, A. Woyte, J. Driesen, and R. Belmans, "A Voltage and Frequency Droop Control Method for Parallel Inverters," *IEEE Transactions on Power*

Electronics, vol. 22, no. 4, pp. 1107–1115, Jul. 2007. https://doi.org/10.1109/tpel.2007.900456

[5] S. Nourollah, A. Pirayesh, and F. Aminifar, "Combinational scheme for voltage and frequency recovery in an islanded distribution system," *IET Generation, Transmission & Distribution*, vol. 10, no. 12, pp. 2899–2906, Sep. 2016. https://doi.org/10.1049/iet-gtd.2015.1302

[6] S. Krishnamurthy, T. M. Jahns, and R. H. Lasseter, "The operation of diesel gensets in a CERTS microgrid," *2008 IEEE Power and Energy Society General Meeting - Conversion and Delivery of Electrical Energy in the 21st Century*, Jul. 2008, pp. 1–8. https://doi.org/10.1109/pes.2008.4596500

[7] Y. Zhang, R. Xiong, H. He, and W. Shen, "Lithium-Ion Battery Pack State of Charge and State of Energy Estimation Algorithms Using a Hardware-in-the-Loop Validation," *IEEE Transactions on Power Electronics*, vol. 32, no. 6, pp. 4421–4431, Jun. 2017. https://doi.org/10.1109/tpel.2016.2603229

[8] M. Ceci, R. Corizzo, F. Fumarola, D. Malerba, and A. Rashkovska, "Predictive Modeling of PV Energy Production: How to Set Up the Learning Task for a Better Prediction?," *IEEE Transactions on Industrial Informatics*, vol. 13, no. 3, pp. 956–966, Jun. 2017. https://doi.org/10.1109/tii.2016.2604758

[9] G. Sideratos and N. D. Hatziargyriou, "An Advanced Statistical Method for Wind Power Forecasting," *IEEE Transactions on Power Systems*, vol. 22, no. 1, pp. 258–265, Feb. 2007. https://doi.org/10.1109/tpwrs.2006.889078

[10] H.-T. Yang, C.-M. Huang, Y.-C. Huang, and Y.-S. Pai, "A Weather-Based Hybrid Method for 1-Day Ahead Hourly Forecasting of PV Power Output," *IEEE Transactions on Sustainable Energy*, vol. 5, no. 3, pp. 917–926, Jul. 2014. https://doi.org/10.1109/iciea.2014.6931220

[11] A. Dolara, S. Leva, M. Mussetta, and E. Ogliari, "PV hourly day-ahead power forecasting in a micro grid context," *2016 IEEE 16th International Conference on Environment and Electrical Engineering (EEEIC)*, Jun. 2016, pp. 1–5. https://doi.org/10.1109/eeeic.2016.7555636

[12] Y. Hosoda and T. Namerikawa, "Short-term photovoltaic prediction by using H∞ filtering and clustering," *2012 Proceedings of SICE Annual Conference (SICE)*, Akita, 2012, pp. 119–124.

[13] A. Shakya, S. Michael, C. Saunders, D. Armstrong, P. Pandey, S. Chalise, and R. Tonkoski, "Solar Irradiance Forecasting in Remote Microgrids Using Markov Switching Model," *IEEE Transactions on Sustainable Energy*, vol. 8, no. 3, pp. 895–905, Jul. 2017. https://doi.org/10.1109/tste.2016.2629974

[14] "IREN2", [Online]. Available: http://www.iren2.de

[15] R. Köberle, K. Mayr, B. Rindt, T. Sowa, D. Buchstaller, A. Armstorfer, and H. Biechl, "IREN2: Zukunftsfähige Netze zur Integration Regenerativer Energiesysteme," in *ETG-Fb. 145: Von Smart Grids zu Smart Markets 2015*, 2015.

[16] A. Armstorfer, H. Biechl, B. Alt, H. Müller, R. Sollacher, D. Most, A. Szabo, R. Köberle, and M. Fiedeldey, "Einsatz von Batteriespeichern in Smart Grids – Operation of Battery Storage Systems in Smart Grids," *Int. ETG-Kongress*, pp. 1–8, 2013.

Andreas Armstorfer received his Dipl. ing. (FH) and M.Eng. degree from Kempten University of Applied Sciences in 2011 respectively 2015. Since 2011 he is working as a researcher at the Institute of Electrical Power Systems (IEES) of the University of Applied Sciences Kempten and is currently a PhD student at Tallinn University of Technology, Estonia.

His main research focus is on modeling, simulation and control as well as stability analysis of Micro Grids with a high penetration of renewable energy sources taking into account inverters, rotating machines as well as battery storage systems.

Postal address: University of Applied Sciences Kempten, Institute of Electrical Power Systems (IEES), Bahnhofstrasse 61, 87435 Kempten, Germany.

Helmuth Biechl received his Dipl. ing. Univ. and M.Sc. degree from the Technical University of Munich (TUM) in 1985 and his Dr. ing. and PhD degree in 1989 also from the Technical University of Munich. From 1989 till 1994 he was a developing and planning engineer and a group leader at the companies Siemens and E.ON.

Since 1994 he is a full professor at the University of Applied Sciences Kempten in Germany and working on the field of electrical power systems, mainly electrical machines, drives, power transmission and distribution systems including batteries for power engineering application. Since 2011 he is the Director of the Institute of Electrical Power Systems (IEES). Since 2005, he is a Titular Professor at the Universidad Pontificia Bolivariana in Colombia where he got a doctor honoris causa degree in 2012. His main research interests are modeling, simulation and optimization of electrical power systems. He has published more than 40 international scientific papers and about 200 articles in technical magazines.

Postal address: University of Applied Sciences Kempten, Institute of Electrical Power Systems (IEES), Bahnhofstrasse 61, 87435 Kempten, Germany.

Argo Rosin received the Dipl. Eng., M.Sc. and Dr.sc.techn. degrees in electrical engineering from Tallinn University of Technology (TUT), Tallinn, Estonia, in 1996, 1998 and 2005, respectively. He is presently a Senior Researcher in the Department of Electrical Power Engineering and Mechatronics, TUT. He has published more than 70 scientific papers on energy management, control and diagnostic systems development and is the holder of a Patent in this application field. His research interests include modelling and simulation of power management and industrial control systems. He is member of IEEE Industrial Electronics Society, IEEE Power & Energy Society, and Estonian Association of Engineers.

Postal address: School of Engineering, Tallinn University of Technology, Ehitajate str. 5, 19086 Tallinn, Estonia.